Bearing capacity of reinforced soil under a strip footing: centrifuge tests

Alexandros Kyparissis
A-Squared Engineers, United Kingdom

Margarida Pinho-Lopes
University of Southampton, United Kingdom

ABSTRACT: Geosynthetics can be used to increase the bearing capacity of poor foundation soils and/or to reduce excessive settlements. This paper analyses the case of shallow foundations on reinforced soil using centrifuge tests, namely that of a strip footing on a horizontal ground reinforced with one layer of geosynthetic. The response of reinforced models was compared to that of a similar unreinforced model. The influence of the depth of the reinforcement layer was studied. Two different reinforcement materials were used: a geotextile and a geogrid. The ultimate bearing capacity, as well as the bearing capacity at particular settlement levels were analysed. The results indicate that using one layer of reinforcement contributes to increasing the ultimate bearing capacity, provided the reinforcement is adequately positioned. It is likely that the higher limit for the normalized depth of the reinforcement layer recommended in the literature may need to be reduced, when using only one layer of reinforcement. The improvement in bearing capacity at particular settlement levels is important as often the settlement, rather than the bearing capacity, controls design. The models tested exhibited reduced bearing capacity for normalised settlements of 5%B (B, width of the footing), while for smaller normalised settlements (2%B) the reinforcement layer included was effective, particularly when the reinforcement layer was placed nearer to the footing. The experimental data was compared to analytical estimates of the bearing capacity with proposals from the literature. The analytical estimates are optimistic, particularly for the geogrid.

Keywords: centrifuge tests, strip foundation, reinforced soil, geosynthetic, bearing capacity

1 INTRODUCTION

Geosynthetics have been used to increase the bearing capacity of poor foundation soils and/or to reduce excessive settlements. Particular attention has been given to the case of shallow foundations on reinforced soil. Several authors have studied this problem using experimental, numerical and/or analytical approaches (Sharma et al. 2009). The experiments reported in the literature included a wide range of soils (sandy soils, clayey soils, aggregates and pond ash).

Experimental studies available in the literature allow distinguishing two fundamental reinforcing mechanisms contributing to the increase in bearing capacity of reinforced soil foundations: confinement effect and membrane effect (Chen and Abu-Farsakh 2015). For the first mechanism, as loads are applied, lateral forces are induced in the soil, which cause horizontal deformations. Such movements originate relative displacements between the soil and the reinforcements, mobilising the interface resistance. Therefore, lateral confinement is introduced that leads to increased compressive strength of the soils, improving their bearing capacity. The second mechanism refers to the deformations and tensions induced on the reinforcement due to the settlement of the soil below a footing. An upward force mobilised in the deformed reinforcement supports part of the load applied by the footing. For this mechanism to develop it is necessary that some settlement occurs and that the length and the tensile strength of the reinforcement are adequate to prevent pull-out and tensile failures.

Three potential failure modes of reinforced soil foundations have been identified (Chen and Abu-Farsakh 2015): a) failure above the top layer of reinforcement; b) failure between layers of reinforcement;

c) punching shear failure followed by a general shear failure. The notation used is as follows: B, width of the footing; u, depth of the first layer of reinforcement; h, vertical spacing between consecutives layers of reinforcement; d_r, depth of the reinforced zone contributing to the bearing capacity; l, effective length of the reinforcement. The failure above the top layer of reinforcement will be more likely when the first layer of reinforcement is sufficiently deep (u>0.5B). The failure between layers of reinforcement will tend to occur for large spacing between reinforcement layers (h>0.5B). Chen and Abu-Farsakh (2015) point out that the relevance of the punching shear failure (within the third failure mode) is often represented by the punching shear failure depth (D_p), which in turn depends on the relative strength of the unreinforced and reinforced zones. D_p will range between 0 and d_r: D_p=0 for situations where the strength difference between the reinforced zone and the underlying unreinforced zone is small or the reinforcement depth ratio (d_r/B) is relatively large; D_p=d when the strength ratio between the reinforced zone and the unreinforced area below is large or for relatively small reinforcement depth ratio.

The information available in the literature has allowed defining guidelines for distributing reinforcement layers beneath footings on horizontal ground. For example, Sharma et al. (2009) summarised results from the literature to define the reinforcement layout: depth of first layer of reinforcement, u: 0.2B – 0.5B; vertical spacing between consecutive layers of reinforcement, h: 0.2B – 0.5B; maximum total depth of reinforced areas, d: 1.0B – 2.0B; effective length of reinforcement, l: 2.0B – 8.0B. Most of the experimental studies in the literature are based on small-scale models. For other problems, such as slopes in reinforced soil several authors have used centrifuge tests (Hu et al. 2010, Raisinghani and Viswanadham 2011, Wang et al. 2011). Although they can be expensive and time consuming, centrifuge models tests can reproduce the stress level, deformations and failure mechanisms observed in a prototype structure (Wang et al. 2011).

Michalwoski (2004) proposed equations to estimate the bearing capacity of reinforced soils. Two cases were considered: 1) the reinforcement layers slip within the soil (the bearing capacity depends on the soil-reinforcement interface properties); 2) the reinforcement ruptures (the bearing capacity depends on the strength of the reinforcement).

To contribute to addressing the limitations of published studies on footings on reinforced soil based on small-scale model tests, this paper reports a series of centrifuge tests. The problem analysed is that of a strip footing on a reinforced soil foundation with horizontal surface. The bearing capacity of the reinforced models is compared to that of the unreinforced solution. The improvement in bearing capacity at particular settlement levels is also analysed, as often the settlement, rather than the bearing capacity, controls design.

2 EXPERIMENTAL PROGRAMME

This paper reports centrifuge tests of a strip footing on reinforced soil, as well as initial tests to characterise the soil and the reinforcements, and their interface (using direct shear tests).

2.1 *Soil*

The soil used on the centrifuge tests was a fine uniform sand (Table 1). The strength parameters of the soil (peak and constant volume angle of friction, ϕ'_p and ϕ'_{cv}, respectively) were determined from direct shear tests (according to BS 1377-7:1990), for confining stresses of 50 kPa, 100 kPa and 150 kPa. In all tests, the sand was dry and compacted for a relative density (I_D) of 97%.

Table 1. Properties of the sand tested.

D_{min}	D_{10}	D_{30}	D_{50}	D_{60}	D_{max}	C_u	C_c	G_s	e_{max}	e_{min}	ϕ'_p	ϕ'_{cv}	I_D
(mm)	(mm)	(mm)	(mm)	(mm)	(mm)	(-)	(-)	(-)	(-)	(-)	(°)	(°)	(%)
0.125	0.170	0.195	0.200	0.230	0.355	1.2	0.9	2.7	0.82	0.63	31.7	26.2	97

2.2 *Reinforcements*

Two types of model reinforcements were used in the centrifuge tests (Figure 1):

- GTX_m, a continuous nonwoven material (representing a geotextile on prototype);
- GGR_m, a fibreglass mesh with a grid structure (representing a geogrid on prototype).

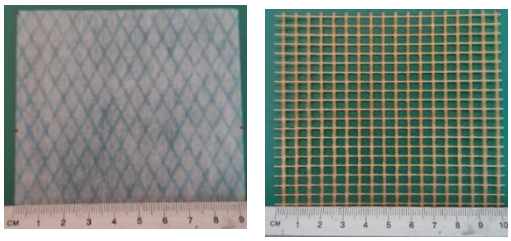

a) b)

Figure 1. Model geosynthetics used in the centrifuge tests: a) GTX_m, geotextile; b) GGR_m, geogrid.

GTX_m was formed via mechanical bonding of small fibres. The material is anisotropic and two perpendicular directions were identified, relatively to the orientation of its fibres: direction A, parallel to the length of the fibres; direction B, perpendicular to the fibres. Two differently sized ribs placed perpendicularly, which result in an anisotropy of strength, form GGR_m. The model geogrid was supplied in a roll, thus the terminology used for prototype geosynthetics was adopted to distinguish two directions within the model geogrid: machine direction (MD), along the roll; cross-machine direction (CD), perpendicular to the machine direction (along the width of the roll). To characterise the model reinforcements, tensile tests were performed following the procedures described in EN ISO 10319:2008. Table 2 summarises relevant properties of the model reinforcements: thickness, d; mass per unit area, ρ_A; tensile strength, T_{max}, and corresponding strain, ε_{max}, force for 1% and 2% strain, $T_{1\%}$ and $T_{2\%}$, respectively.

Table 2. Properties of the model reinforcements used on the centrifuge tests.

Material	d (mm)	ρ_A (g/m^2)	Openings (mm^2)	Direction	T_{max} (kN/m)	ε_{max} (%)	$T_{1\%}$ (kN/m)	$T_{2\%}$ (kN/m)
GTX_m	0.20	29.5	-	A	1.41	9.58	0.47	0.76
				B	0.16	7.75	0.09	0.11
GGR_m	-	147.4	4 x 4	MD	3.42	1.79	2.81	3.00
				CMD	4.44	1.59	2.60	2.60

The soil-reinforcement interface strength was characterised using direct shear tests. The procedures were based on EN ISO 12957-1:2005; however, the tests were performed in a small box (as for the sand): plan section 100 x 100 mm^2, total height 25 mm. For each interface, 4 specimens were tested, for confining stresses of 50 kPa, 100 kPa (2×) and 150 kPa. Table 3 summarises the results as angle of friction of the soil-reinforcement interface for zero intersect, δ^*, and interface friction ratio, R_{inter} ($\tan \delta^*/\tan \phi'$).

Table 3. Peak and constant volume (CV) soil-reinforcement interface friction angle, δ^*, and friction ratio, R_{inter}.

Reinforcement	δ^* (°)		R_{inter}	
	Peak	CV	Peak	CV
GTX_m	30.3	25.5	0.95	0.97
GGR_m	30.3	25.1	0.95	0.95

2.3 *Centrifuge tests*

The physical modelling was performed on the geotechnical centrifuge of the University of Brighton, UK (Figure 2). This is a beam centrifuge with a radius of rotation of 0.66 m, with swing buckets installed at the end of the beams. The system has a maximum rotational velocity of 638 rpm and it can subject a model to an acceleration field of up to 300g. The strongboxes used are made of steel with acrylic walls, to provide visual access to the specimens' profile during flight. The internal dimensions of the strongbox allowed samples of 0.30 m in length, 0.10 m in width and 0.18 m in height. Loads are applied to the models using a strain-controlled actuator (Figure 2c). The total height of the soil was 160 mm, to allow for the footing and the actuator's rod to settle together inside the strongbox. The model strip footing was made of steel, with dimensions of 0.025 m in width, 0.095 m in length and 0.010 m in thickness. The footing included a recess (centred) to accommodate a ball bearing, which was used to decrease any eccentricity

when the footing was loaded. Finally, sandpaper was glued on the bottom part of the footing in order to increase the friction between the soil and the footing and prevent it from translating in case eccentric loading would occur.

The relative position of the reinforcement layer was defined using values normalised to the width of the footing (B). Three values for the normalised depth of the reinforcement layer, u/B, were considered (all within the range proposed in the literature): 0.25, 0.35 and 0.50 (corresponding to depths of 6.25 mm, 8.75 mm and 12.5 mm; for B=25 mm). The reinforcement layer had the same length in all the models (100 mm), defined as 4 times the width of the footing (l=4B), as proposed by Latha and Somwanshi (2009).

The experimental programme included testing an unreinforced model (U) and reinforced models including one layer of GTX_m or GGR_m placed at different depths (Figure 2d). In total 7 centrifuge models are reported. Additional tests to check the repeatability of the results were performed (not included herein).

The models were built in layers at 1g, to the desired relative density. The sand was poured into the strongbox in layers and it was vibrated; the reinforcement layer was placed at the desired depth with the same sand coloured on top. Then the model was installed on the centrifuge beam, the centrifuge tank was sealed and rotation was initiated to 30g (202 rpm). Once the desired acceleration was achieved, the actuator was enabled and a loading rate of 2 mm/minute was applied, until failure.

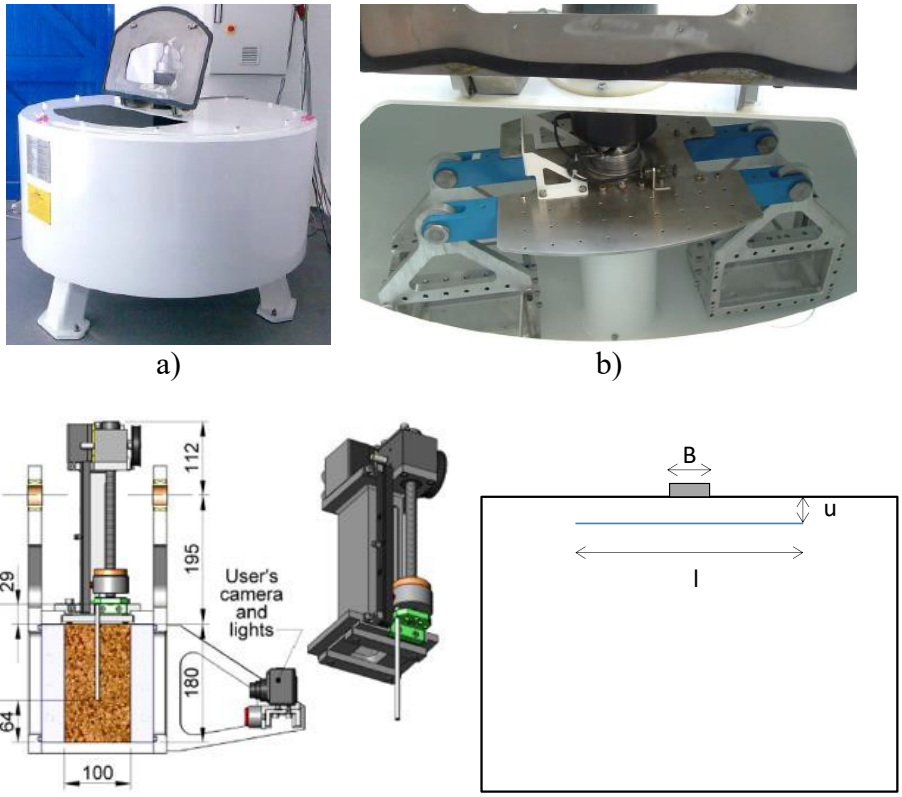

Figure 2. a) Geotechnical centrifuge at the University of Brighton, b) interior of the geotechnical centrifuge with strongboxes equipped on the ends of the beam; c) centrifuge strongbox equipped with acrylic walls, actuator and digital camera placement (dimensions in mm) (courtesy of Thomas Broadbent and Sons Limited®); d) schematic configuration of the centrifuge tests.

3 RESULTS AND DISCUSSION

The test results are summarised and discussed. Analytical equations from the literature were used to quantify the contribution of the reinforcements; the influence of the depth of the reinforcement layer is analysed.

3.1 *Summary of results*

Table 4 summarises some test results; additional tests were carried out to ensure repeatability of results (not reported herein as they all are in good agreement). Figures 3 and 4 illustrate the normal pressure ver-

sus normalised settlement of the footing obtained for the different tests, for GTX_m and GGR_m, respectively. There was some noise in the data, which is related to the electronic wiring of the actuator passing near the slip rings (located inside the centrifuge's rotational axis), which produces a magnetic field when the centrifuge operates. However, the response of the models is defined clearly. The curves exhibited an initial region of settlement without significant variation in the applied pressure. The actuator was not in direct contact with the ball bearing at the initiation of the test. At the beginning of each test, some time was required for the shaft to reach the ball bearing and start loading the footing. Thus, as it did not reflect the response of the model, the corresponding parts of the curves were removed for clarity.

Table 4. Centrifuge testing program and summary of results.

Designation	Reinforcement		Summary of results			
	Material	Depth of layer	Pressure s=2%B	Pressure s=5%B	Maximum pressure, 1st peak	Maximum pressure, 2nd peak
		u/B	$q_{s=2\%B}$	$q_{s=5\%B}$	$q_{max,1}$	$q_{max,2}$
		(-)	(kPa)	(kPa)	(kPa)	(kPa)
U	-	-	35.8	131.0	199.2	-
R_GTX_1_25	GTX_m	0.25	34.5	105.4	285.5	-
R_GTX_1_35		0.35	40.5	112.7	281.6	281.6
R_GTX_1_50		0.50	32.8	96.1	130.8	359.0
R_GGR_1_25	GGR_m	0.25	44.9	130.8	224.6	-
R_GGR_1_35		0.35	40.9	111.8	219.9	224.3
R_GGR_1_50		0.50	40.0	159.4	195.4	337.5

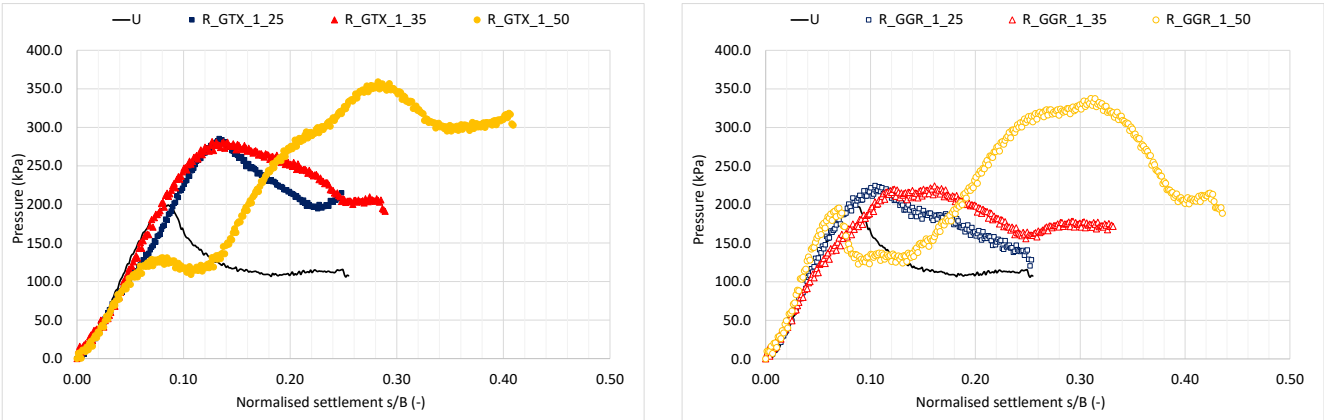

a) b)

Figure 3. Pressure versus normalised settlement for models reinforced with: a) GTX_m; b) GGR_m.

The response of the models was also analysed by comparing the bearing capacity ratio (BCR), defined using Equation 1, suggested by Binquet and Lee (1975), as the ratio between the bearing capacity of the reinforced soil model ($q_{u(R)}$) to that of the unreinforced model ($q_{u(UR)}$).

$$BCR = \frac{q_{(R)}}{q_{(UR)}} \tag{1}$$

To quantify the influence of the reinforcement layer, different BCR values were defined, using the data presented in Table 4. Thus, two peak values were defined (one per peak, BCR_{max1} and BCR_{max2}), and two for normalised footing settlements of 2%B and 5%B ($BCR_{2\%B}$ and $BCR_{5\%B}$, respectively). The reinforcements used in the tests do not have the same tensile strength or stiffness and they have different structures; thus, the results for similar test conditions are not directly compared.

3.2 *Influence of the depth of the reinforcement layer*

Initially, the unreinforced model had an approximately linear response, followed by a peak in pressure. The response of the reinforced models is qualitatively similar to that of the unreinforced one, with the exception of the models where u/B=0.5. Those models (reinforcement layer at a normalised depth u/B=0.5) failed prematurely relatively to the unreinforced model, indicating there was a localised failure above the reinforcement. However, as the reinforcements were sufficiently long (l/B=4), they were mobilised and additional strength developed, increasing the bearing capacity of the models. Nevertheless, the maximum applied pressure was mobilised at very high normalised settlements (29% and 31%, respectively, for the models reinforced with GTX_m and GGR_m at u/B=0.5). These results indicate that, for conditions similar to the ones reported herein, the limiting depth at which the reinforcement is placed should be smaller than the limit recommended in the literature u/B=0.5.

The models with the reinforcement layer at lower depth (u/B=0.25 and u/B=0.35) were able to withstand higher pressures than the unreinforced model, for higher settlement of the footing. It is likely that the two reinforcing mechanisms (confinement and membrane effects) described before were mobilised by each reinforcement, although differently. The geogrid structure allows soil particles to move vertically within the openings, while the geotextile (sheet material) restrains those movements, acting as a separator between the soil above and beneath the reinforcement. This (together with the different stiffness of the reinforcements) affects the mobilisation of each reinforcement.

Figure 4 summarises the bearing capacity ratio, BCR, for the two types of reinforcements analysed (for different values of the normalised depth of the reinforcement layer). Figure 4a refers to the peak values (BCR_{max1} and BCR_{max2}), while Figure 4b refers to normalised footing settlement of 2%B and 5%B ($BCR_{2\%B}$ and $BCR_{5\%B}$, respectively). The results indicate that when the reinforcement layer was placed at smaller depths (u/B=0.25 or 0.35) there was an increase in the ultimate bearing capacity of the reinforced soil foundation relatively to the unreinforced solution (BCR_{max1}=BCR_{max2} between 1.1 and 1.4), for both the geotextile and the geogrid. However, for smaller normalised settlement (2%B and 5%B), a different trend was observed. For 2%B normalised settlement, the reinforcement was effective in increasing the BCR ($BCR_{2\%B}$ between 1 and 1.3), except for the model GTX_1_0.25, with $BCR_{2\%B}$=0.9). The increase in $BCR_{2\%B}$ may be caused by pre-tensioning of the reinforcement during assembly of the models. For larger settlements, particularly for a settlement of 5%B, introducing the reinforcement layer reduced the $BCR_{5\%B}$ (in most cases <1.0). For the reinforcements to be further mobilised, they undergo deformations induced by the settlements imposed during the tests.

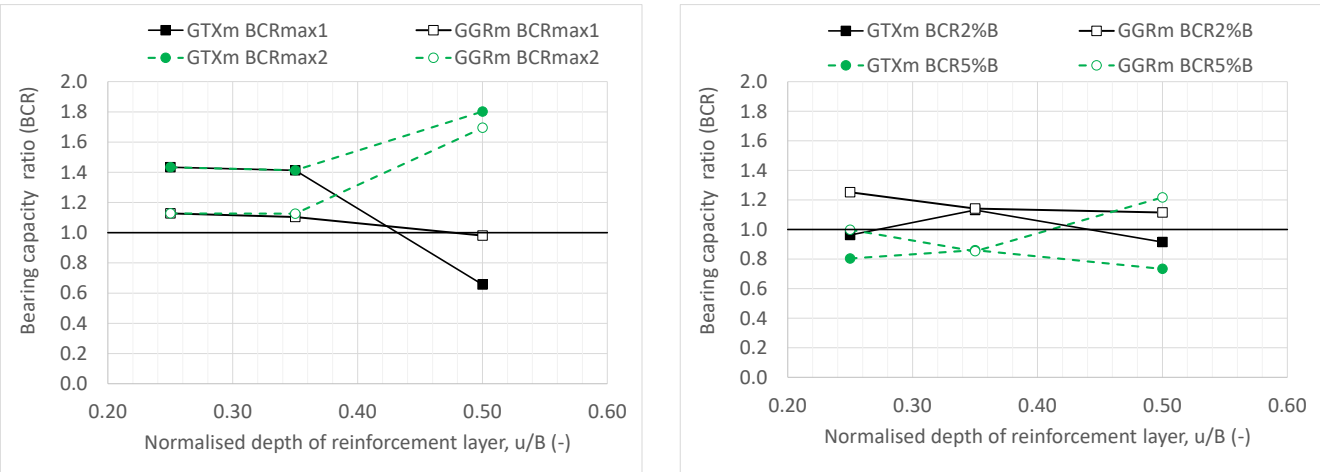

a) b)

Figure 4. Bearing capacity ratio (BCR) for: a) the first and second peak in applied pressure (BCR_{max1} and BCR_{max2}); b) an imposed settlement of 2% and 5% ($BCR_{2\%B}$ and $BCR_{5\%B}$).

4 EXPERIMENTAL DATA VERSUS ANALYTICAL SOLUTIONS

The experimental results were compared with analytical estimates for the bearing capacity. The ultimate bearing capacity of the unreinforced soil was estimated using Equations 2 to 4.

$$q_{u(UR)} = \frac{1}{2}\gamma B N_\gamma \tag{2}$$

$$N_\gamma = 2\left(N_q - 1\right)\tan(\phi) \tag{3}$$

$$N_q = e^{\pi \tan\phi} \tan^2\left(\frac{\pi}{4} + \frac{\phi}{2}\right) \tag{4}$$

The theoretical bearing capacity obtained (67kPa) is very conservative when compared to the value obtained from the centrifuge tests (199kPa). This is inherent of the equation used; additionally, the angle of friction estimated from the direct shear tests is likely to be a low estimate. Using a value of ϕ=32° (more realistic for the sand used) would result in a more realistic bearing capacity $q_{u(UR)}$=169kPa (Table 5).

The bearing capacity of the reinforced soil was estimated using Equations 5 and 9 by Michalowski (2004). Equation 5 refers the case where the reinforcement layers slip within the soil and is only valid when the failure mechanism forms above the reinforcement layer, while Equation 9 refers to the tensile failure of the reinforcement. Here, μ = interface friction coefficient, taken as a fraction (f_b) of tanϕ, T_t = tensile strength of the reinforcement; Equation 6 is an approximation for one layer of reinforcement.

$$q_{u(R)} = \frac{1}{1-\mu\frac{u}{B}M_p}\left[\gamma B\left(\frac{1}{2}N_\gamma + \mu\frac{u}{B}M\right)\right] \tag{5}$$

$$M = 1.6(1 + 8.5\tan^{1.3}\phi) \tag{6}$$

$$M_p = 1.5 - 1.25 \times 10^{-2}\,\phi, \text{ with } \phi \text{ in degrees} \tag{7}$$

$$\mu = f_b \tan\phi \tag{8}$$

$$q_{u(R)} = \frac{1}{2}\gamma B N_\gamma + \frac{T_t}{B}M_r \tag{9}$$

$$M_r = (1 + \sin\phi)e^{\left(\frac{\pi}{2}+\phi\right)\tan\phi} \tag{10}$$

Table 5. Summary of results from analytical solutions (Michalowski 2004).

Designation	Reinforcement		Summary of results					
	Material	Depth of layer	ϕ=26.2°			ϕ=32°		
		u/B	$q_{u(UR)}$ or $q_{u(R)}$ (Eq. 5)	$q_{u(UR)}$ or $q_{u(R)}$ (Eq. 9)	BCR	$q_{u(UR)}$ or $q_{u(R)}$ (Eq. 5)	$q_{u(UR)}$ or $q_{u(R)}$ (Eq. 9)	BCR
		(-)	(kPa)	(kPa)	(-)	(kPa)	(kPa)	(-)
U	-	0	66.8	66.8	1.00	169.4	-	1.00
R_GTX_1_25	GTX_m	0.25	89.6	287.4	1.33	223.3	506.5	1.31
R_GTX_1_35		0.35	100.9	287.4	1.50	251.4	506.5	1.47
R_GTX_1_50		0.50	121.2	287.4	1.79	304.0	506.5	1.77
R_GGR_1_25	GGR_m	0.25	89.0	601.8	1.33	221.9	971.8	1.31
R_GGR_1_35		0.35	100.0	601.8	1.50	249.2	971.8	1.47
R_GGR_1_50		0.50	119.7	601.8	1.79	299.9	971.8	1.77

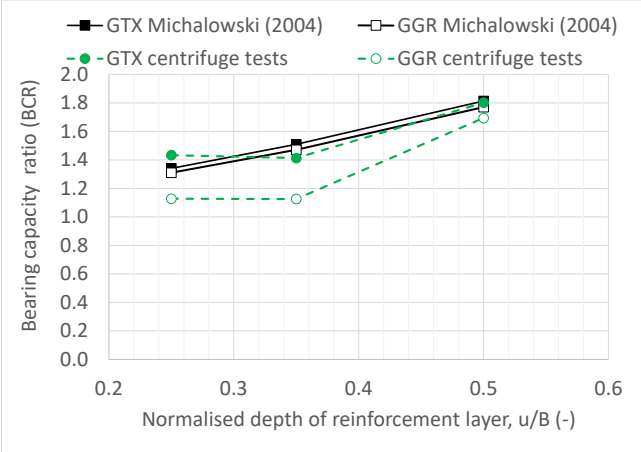

Figure 5. Bearing capacity ratio (BCR) obtained from the centrifuge tests (BCR_{max2}) and the analytical predictions (Equation 5, ϕ=32°).

For the reinforced cases, the critical failure mode is the slip of the reinforcement within the soil. This is in agreement with the experimental data, as no tensile failure of the reinforcement layers was observed. When considering the angle of friction of the soil ϕ=32°, the analytical estimates of the bearing capacity give a good, though mostly optimistic, approximation of the bearing capacity of the reinforced soil, particularly for the maximum bearing capacity (identified in Table 4 as the 2nd peak). Figure 5 compares the experimental results (BCR_{max2}) with the analytical estimates for ϕ=32° (Equation 5). The equations seem to capture the maximum bearing capacity of GTX, while for GGR the analytical estimates are optimistic.

5 CONCLUSIONS

In this paper, the bearing capacity of a strip footing on a reinforced soil foundation with horizontal surface was analysed. A series of centrifuge tests were performed and the response of the models reinforced with one layer of geosynthetic was compared to that of the unreinforced model tested under the same conditions. Besides the ultimate bearing capacity, the improvement in bearing capacity at particular settlement levels was also analysed.

The results indicate that using one layer of reinforcement contributes to an increase of the ultimate bearing capacity, provided the reinforcement is adequately positioned. It is likely that the higher limit for the normalized depth of the reinforcement layer recommended in the literature (u/B=0.5) may need to be reduced, when using only one layer of reinforcement. The improvement in bearing capacity at particular settlement levels is important as often the settlement, rather than the bearing capacity, will control design. The models tested exhibited reduced bearing capacity for normalised settlements of 5%B, while for smaller normalised settlements (2%B) the reinforcement layer included was effective, particularly for layers placed near the footing.

The analytical estimates using the equations proposed by Michalowski (2004) agree with the experimental data on the high resistance to tensile failure. Additionally, the maximum bearing capacity observed in the centrifuge tests was estimated reasonably, particularly for the geotextile. For the geogrid the predictions are optimistic. Nevertheless, the equations cannot predict the qualitatively pressure-settlement response observed for u/B=0.5, with two peaks.

ACKNOWLEDGMENTS

The authors would like to thank the Geotechnical Laboratory of University of Brighton, UK, where the experiments were done, particularly Dr Jerome Le Cossec for his support.

REFERENCES

Binquet, J. & Lee, K.L. 1975. Bearing capacity analysis on reinforced earth slabs. J. Geotech. Eng. Div., Vol. 101 (GT12), pp. 1257–1276.

BSI (2008) EN ISO 10319:2008: Geosynthetics. Wide-width tensile test. BSI, London, UK.

BSI (2005) EN ISO 12957-1:2005: Geosynthetics -- Determination of friction characteristics -- Part 1: Direct shear test. BSI, London, UK.

Chen, Q. & Abu-Farsakh, M. 2015. Ultimate bearing capacity analysis of strip footings on reinforced soil foundation. Soils and Foundations, Vol 55(1), pp. 74-85.

Hu, Y., Zhang, G., Zhang, J.-M. & Lee, C.F. 2010. Centrifuge modelling of geotextile-reinforced cohesive slopes. Geotextiles and Geomembranes, Vol. 28(1), pp. 12-22.

Latha, G.M. & Somwanshi, A. 2009. Bearing capacity of square footings on geosynthetic reinforced sand. Geotextiles and Geomembranes, Vol. 27(4), pp. 281-294.

Michalowski, R.L. 2004. Limit Loads on Reinforced Foundation Soils. Journal of Geotechnical and Geoenvironmental Engineering ASCE, Vol. 130(4), pp. 381-390.

Raisinghani, D.V. & Viswanadham, B.V.S. 2011. Centrifuge model study on low permeable slope reinforced by hybrid geosynthetics. Geotextiles and Geomembranes, Vol. 29(6), pp. 567-580.

Sharma, R., Chen, Q., Abu-Farsakh, M. & Yoon, S. 2009. Analytical modeling of geogrid reinforced soil foundation. Geotextiles and Geomembranes, Vol. 27(1), pp. 63-72.

Wang, L., Zhang, G. & Zhang, J.-M. 2011. Centrifuge model tests of geotextile-reinforced soil embankments during an earthquake. Geotextiles and Geomembranes, Vol. 29(3), pp. 222-232